THE PADME EXPERIMENT

P. Albicocco (AdR), R. Bedogni, F. Bossi, B. Buonomo, E. Capitolo (Tec.),
C. Capoccia (Tec.), G. Corradi (Tec.), R. De Sangro, G. Finocchiaro, L.G. Foggetta,
G.S. Georgiev (Ass.), A. Ghigo, P. Gianotti (Resp.), V. Kozhuharov (Ass.), M. Palutan,
G. Piperno (AdR), A. Saputi (Tec.), I. Sarra (Ass.), B. Sciascia, T. Spadaro,
E. Spiriti, C. Taruggi (Dott.)

1 Introduction

Direct observations of dark matter signals are necessary to shed light on the cosmological and astrophysical evidences, in order to understand the nature of such unknown matter that at present has manifested itself only via gravitational interactions.

There are models attempting to solve the problem, as well as the muon $(g-2)$ anomaly, that postulates the existence of a low-mass spin-1 particle, named A', that would possess a gauge coupling of electroweak strength to dark matter, and a much smaller coupling to the Standard Model (SM) hypercharge [1]. This Dark Photon (DP) could be the portal connecting ordinary and dark world.

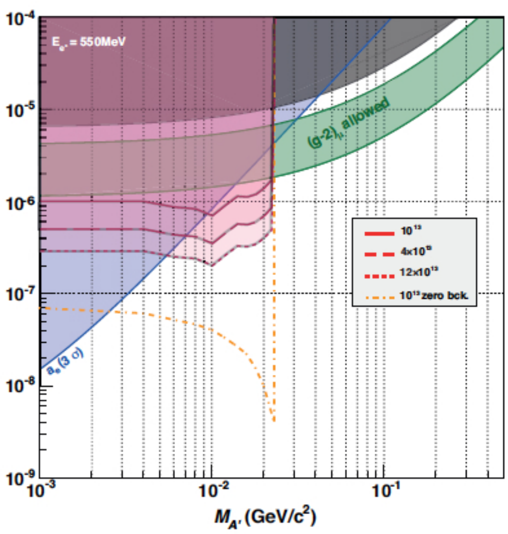

Figure 1: *The PADME experiment sensitivity for various scenarios of recorded luminosity.*

PADME aims to search for signals of this light DP using the positron beam of the LNF LINAC. The experiment, approved by INFN at the end of 2015, will study the reaction:

$$e^+e^- \to \gamma A'$$

and foresees to identify A' by searching for missing mass signals. The PADME physics potential extends beyond DP searches. The detector is also sensitive to any new light particle, including scalars and pseudo-scalars, that are produced in the positron-on-target interaction. An estimate of the physics potential of PADME to search for axion like particles as well as other exotic states is ongoing. In addition, it will be possible to perform measurements of the differential cross sections for Bremsstrahlung emission for positrons in the $O(100\ \text{MeV})$ energy range and to address the multiphoton annihilation cross sections. Presently a sensitivity estimate, based on Monte Carlo simulations, is available only for the invisible DP decays produced by the annihilation process and this is shown in fig. 1. This sensitivity depends crucially on the collected statistics and on the duty cycle of the LINAC. The present beam configuration allows to integrate a total luminosity of 1×10^{13} positrons in 3.15×10^{7} s corresponding to two years data taking at 50% efficiency, but thanks to the modifications implemented to the beam by our collaborators of the LNF Accelerator Division, it is now possible to have bunch lengths up to 200 ns. This new feature will allow to reduce significantly the running time of the PADME experiment.

2 The PADME experiment

The goal of the PADME experiment is to search for DPs produced in the annihilation process of the positron beam of the DAΦNE LINAC with a thin carbon target and then identified using a missing mass technique [2]. The basic elements of the PADME experiment are:

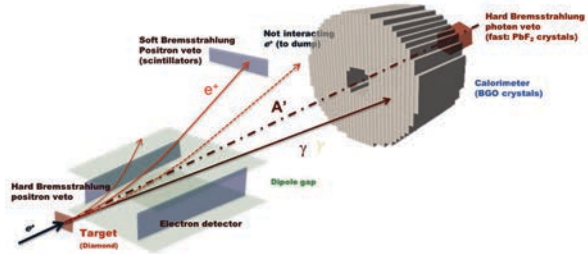

Figure 2: *The PADME experiment concept. From left to right: the active target, the positron/electron vetoes inside a magnetic field, the high energy* e^+ *veto near the non-interacting beam exit, the e.m. calorimeters.*

- a high intensity and low divergence positron beam, impinging on a thin, active target, capable of monitoring the beam spot;
- a vacuum chamber to avoid spurious positron interactions;
- a magnet to deflect the beam of positrons emerging from the target, with the additional task of measuring the momentum of the interacting positrons, thus improving the rejection of the Bremsstrahlung background;
- a finely-segmented, high-resolution e.m. calorimeter, to measure the momentum of the single SM photons;

Since the processes that will mainly take place in the beam-target interaction are Bremsstrahlung and $e^+e^- \to \gamma\gamma(\gamma)$, to cut out these background events, two extra components are crucial:

- a fast Small Angle Calorimeter (SAC), placed behind the central hole of the primary one;

- a charged particle veto system consisting of two modules located inside the dipole magnet gap and a third one on the beam exit.

The layout of the PADME experiment can be seen in fig. 2, while fig. 3 shows a realistic 3D view of the experimental setup.

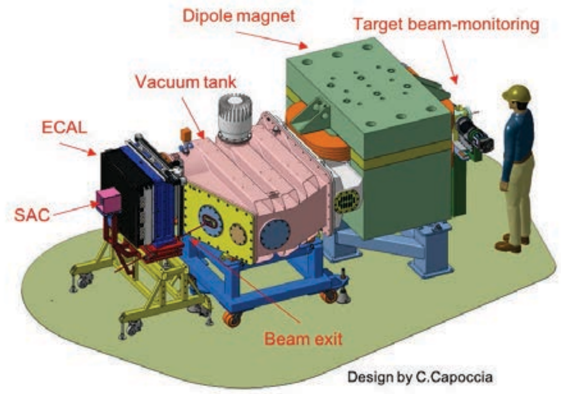

Figure 3: *A CAD drawing of the PADME setup.*

To have a more accurate beam monitoring capability, in the target region will be installed a system based on two planes of silicon pixel detectors placed up and down stream the active diamond target. Each plane will consist of two MIMOSA 28 Ultimate chips, developed for the upgrade of the STAR vertex detector [3]. These devices integrate a Monolithic Active Pixel Sensor (MAPS) with a fast binary readout. Each sensor consists of a matrix of 928×960 pixels of 20.7 μm side with a thickness of 50 μm. For the STAR experiment the chips, that dissipate 150 mW/cm^2, operate in air without cooling. For PADME, the detectors should be placed in vacuum and a modified PCB has been developed by the LNF SEA to provide cooling.

3 Activity of the PADME LNF group

During 2017 the PADME collaboration has worked to complete the design of all detector components and the procurement of the major elements has started.

In the first months of 2017, different data takings were performed at the BTF, in order to test different crystals and photomultipliers for the SAC and the MIMOSA chips necessary for the beam monitoring system. For the SAC, that has to stand rates of MHz, fast crystals are mandatory. To optimize the detector components, different Cherenkov materials and different fast photomultipliers were tested with different beam configurations. The final choice is for PbF_2 crystals (30×30×140 mm^3) coupled to Hamamatsu R13478UV photomultipliers. The obtained energy and time resolutions are shown in fig. 4. These are preliminary results subject to further improvement, since the dimension of the crystal used in the test was not the final one and the coupling with the photomultiplier was therefore not optimal.

The performance of the MIMOSA detector can be seen in fig. 5 where a picture of the BTF electron beam spot, obtained with two different sensors, is visible.

The selection of the main components of the electromagnetic calorimeter (ECAL) was completed in 2016. During all 2017 the LNF group was busy with the tenders for the procurement of

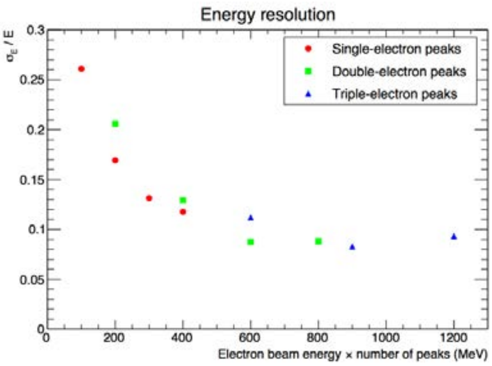

(a)

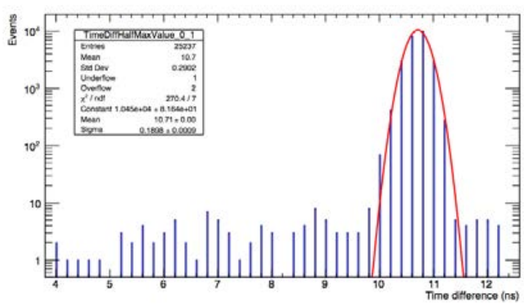

(b)

Figure 4: *Energy (a) and Time (b) resolution obtained during the test beam with a prototype of the SAC crystal (PbF_2).*

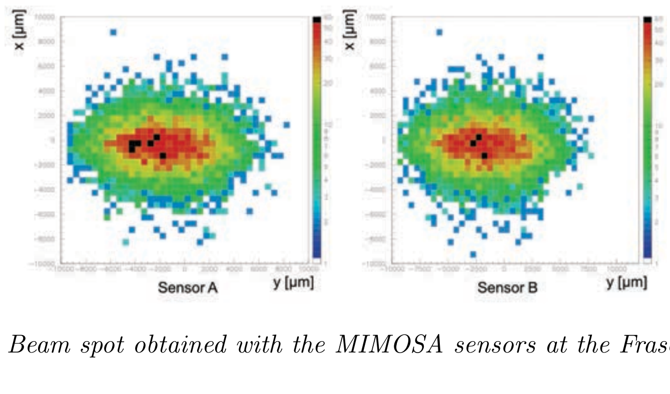

Figure 5: *Beam spot obtained with the MIMOSA sensors at the Frascati BTF.*

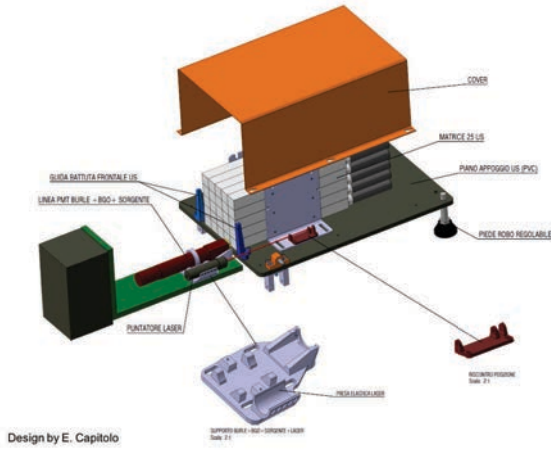

Figure 6: *Setup of the test bench used to calibrate the scintillating units of the ECAL. They consist of BGO crystals (21×21×230 mm^3) withe painted, glued to XP1911 HZC photomultipliers.*

the photosensors and for the reshaping of the BGO crystals, recovered from CERN L3 experiment. The photosensors (HZC XP1911) are glued to the BGO crystals (21×21×230 mm^3) by the same company in charge for the crystal cut and painting. The complete scintillating units started being delivered to LNF at the end of 2017 and they are all characterised in group of 25 with a ^{22}Na radioactive source. The setup of the test bench can be seen in Fig. 6. The source emits two back-to-back gammas of 511 KeV. One, seen by a short BGO crystal, is used to trigger the readout, while the second is entering the scintillating unit under test. The DAQ system collects the charge spectrum of both. With a trigger rate of about 150 Hz, in 3 minute one unit is characterised at a defined value of the photosensor HV. Then, a step motor moves the triggering crystal and the source in front of the second scintillating unit and a new data acquisition is started.

Side of these activities, the design of the mechanical support of the ECAL was carried out. In order to simplify the mechanics, the solution shown in fig. 7 has been adopted. It consists of 616 scintillating units, arranged in a cylindrical matrix, surrounded by "dummy" plastic elements to fill up a squared shape. In this way, the overall support structure could be realized in the INFN internal workshops (Rome3 unit and LNF), saving time and money.

LNF played also a major role in the definition of the final design of the charged particle veto detectors. A special photodetection system, based on SiPMs, was developed by the SEA service. It features a PCB hosting four 3×3 mm^2 SiPMs together with a preamplifier with differential signal outputs and a controller providing the bias voltage and collecting information about the temperature and the current flow through the SiPMs. In addition, an aluminium support structure was built by the main LNF mechanical workshop to hold a set of 16 scintillating bars together with four FEE boards. It served as a mechanical prototype for the final detector construction. During the experiment, FEE boards will be located inside the vacuum chamber and an efficient heat transfer from the SiPMs and the amplifiers to the surface of the vacuum chamber has to be guaranteed. The frame, together with the scintillator bars and the prototype SiPM cards, connected to a prototype of the controller, is shown in fig. 8.

The system was tested with the beam at the BTF in April, 2017. The main goals of this activity were:

- test and choose the best scintillation light collection method, with major choices being either direct light collection or the usage of WLS fibers. The light collection with the WLS fiber

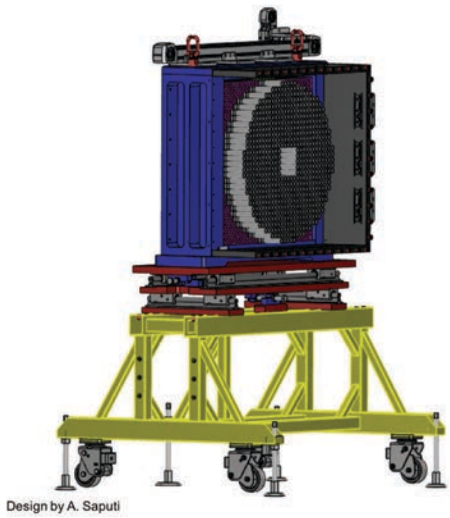

Figure 7: *Mechanical layout of the PADME ECAL. 616 Scintillating units (in grey in the picture) are arranged in a cylindrical array. In the center, a hole of 10×10 cm^2 is foreseen to cut out most of the Bremsstrahlung photons. To simplify the holding structure, dummy plastic elements (in pink in the picture) are placed in the corners. To allow a better view, the left part of the mechanical structure and the back cover are not drawn.*

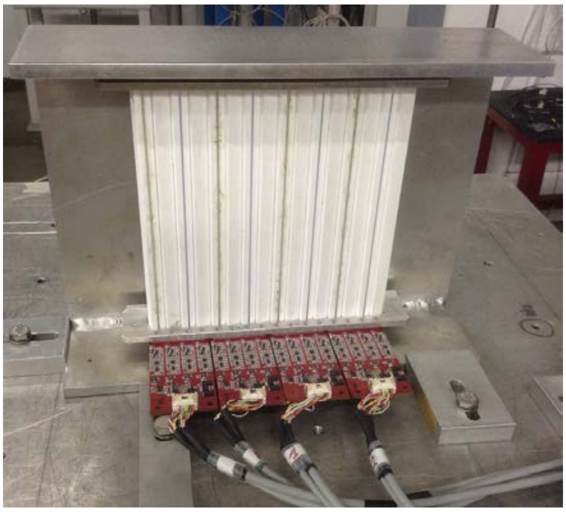

Figure 8: *The charged particle veto prototype placed on the BTF table and prepared for tests.*

turned out to be more insensitive on the crossing point of the particles along the scintillator bars;

- verify the performance of the developed front-end electronics and the chosen photo-sensors. Even if few minor improvable parameters were identified, the general performance of the developed prototype boards demonstrated to comply with the PADME requirements;

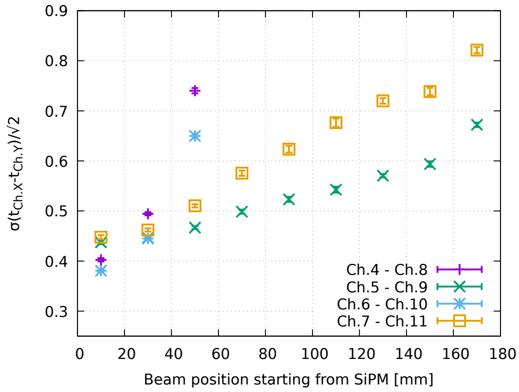

Figure 9: *Time resolution as a function of the impact position of the beam along the scintillator.*

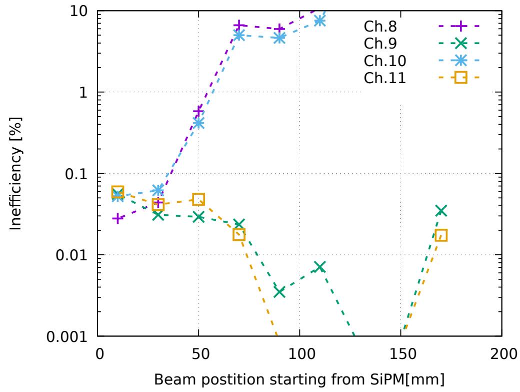

Figure 10: *Inefficiency for charged particle detection.*

- determine the time resolution achievable with different time reconstruction algorithms (shown in fig.9). The time resolution has been of the order of 600 ps, or better, for any impact point along the scintillator;
- measure the efficiency for the detection of charged particles (shown in fig.10). The obtained inefficiency is less than 10^{-3};
- determine the random veto frequency (i.e. the noise) introduced by the individual channels.

The final design of the VETOs has been largely inspired by the prototype design, and was coordinated by LNF technicians. Also the front-end electronics was validated and all the necessary modules have been ordered and delivered to LNF. The final charged particle detectors are currently under construction at the Sofia University and will be delivered at LNF on time for the start of the data taking.

The last activity, carried out at LNF during 2017, has been the complete design of the vacuum system of the experiment. This is separated from the accelerator one by means of a thin Be membrane and after that we can distinguish two zones:

- the target region;
- the vacuum tank.

A CAD drawing of the target region can be seen in fig. 11a. The mechanical components to realize it, have been manufactured by LNF main mechanical workshop. Both the target and the beam monitor are connected to step motors to allow their insertion in and out from the beam line. Fig. 11b shows the beam monitor holder constructed at LNF mechanical workshop following the design realized by SPAS LNF service.

The big vacuum tank (volume ~ 1 m^3) through which the positrons will fly, has been designed by the LNF SPAS service too. It consists of two parts rigidly coupled to form a unique object. The first part, housed inside the dipole, will host mechanical holders for the charged particle veto detectors, while the second one, immediately after the magnet, will end with a circular carbon-fiber flange just in front of the ECAL. On the beam exit path, the third module of the charged particle veto will be installed. The construction of the vacuum tank has been assigned to an external

(a) (b)

Figure 11: *(a) Mechanical layout of the Target region. Two step motors can insert in and out of the beam line both the target and the silicon beam-monitoring system. (b) Mechanical holder of the MIMOSA monitoring system (realized by LNF mechanical workshop).*

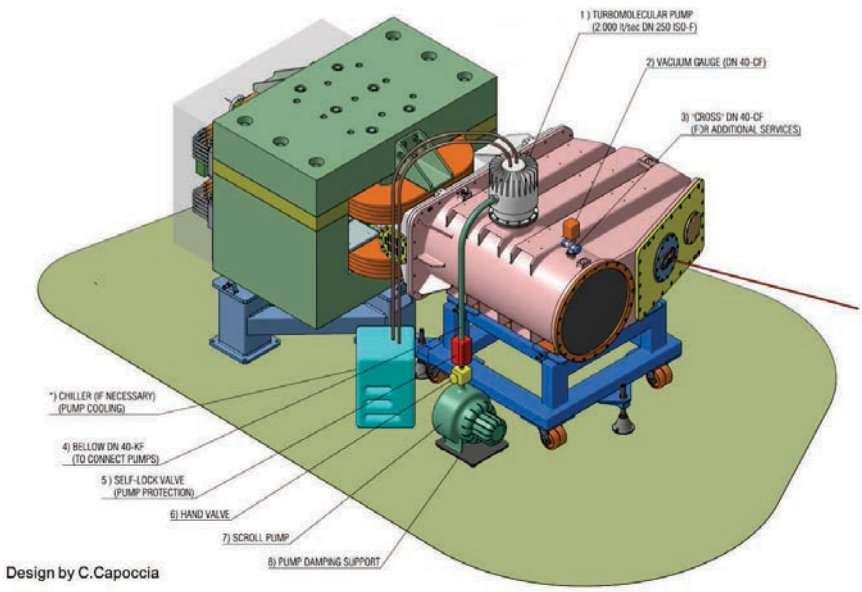

Figure 12: *Layout of the vacuum system of the PADME experiment.*

company as all the cable connector flanges and the exit windows. The delivery of all components is expected in the first quarter of 2018, so that the final assembly in the beam area will be completed to start the data taking between end of April beginning of May 2018.

4 List of Conference Talks by LNF Authors in Year 2017

Here below, it is the list of conference talks given by LNF PADME members:

1. V. Kozhuharov, "PADME: Searching for dark mediator at the Frascati BTF", Les Rencontres de Physique de la Valle d'Aoste, La Thuile, Italy, 5-11 Mar. 2017.
2. G. Piperno, "L'esperimento PADME", XVI Incontri di Fisica delle Alte Energie (IFAE2017), Trieste, Italy, 19-21 Apr. 2017.
3. V. Kozhuharov, "The PADME experiment", II International workshop on Light Dark Matter at Accelerators (LDMA2017), La Biodola, Italy, 24-28 May. 2017.
4. P. Gianotti, "The PADME detector", International Conference on Advancements in Nuclear Instrumentation Measurement Methods and their Applications (ANIMMA2017), Liege, Belgium, 19-23 Jun. 2017.
5. P. Gianotti, "Search for the gauge boson of a secluded sector with the PADME experiment at LNF", EPS Conference on High Energy Physics, Venice, Italy, 5-12 Jul. 2017.
6. G. Piperno, "Dark Photon search with PADME at LNF", Particles and Nuclei International Conference (PANIC 2017), Beijing, China, Sep. 2017.
7. C. Taruggi, "Ricerca di materia oscura presso i LNF: l'esperimento PADME", 103^o Congresso Nazionale SIF, Trento, Italy, 11-15 Sep. 2017.
8. V. Kozhuharov, "A Test System for the Front-End Electronics of the PADME charged particle detector system" XXVI International Scientific Conference Electronics ET 2017, Sozopol, Bulgaria, Sep. 13-15, 2017.
9. G. Georgiev, "Performance of the prototype of the charged particle veto system of the PADME experiment", 14^{th} International Conference on Scintillating Materials and their Applications (SCINT2017), Chamonix, France, 18-22 Sep. 2017.
10. C. Taruggi, "PADME", 13^o Vienna Central European Seminar, Vienna, Austria, 30 Nov. - 1 Dec. 2017.

5 Publications

Here below, it is the list of papers published by PADME LNF members in 2017:

1. V. Kozhuharov, "PADME: Searching for dark mediator at the Frascati BTF ", Nuovo Cim. C40, no.5, (2018) 192.
2. P. Gianotti, "The PADME Detector", EPJ Web Conf. 170 (2018) 01007.
3. M. Raggi *et al.* "The PADME experiment at LNF", EPJ Web Conf. 142, 01026 (2017).
4. E. Leonardi, G. Piperno, M. Raggi, "Evaluation of clustering algorithms at the <1 GeV energy scale for the electromagnetic calorimeter of the PADME experiment", J. Phys. Conf. Ser. 898 (2017) no.7, 072019.

5. E. Leonardi, V. Kozhuharov, M. Raggi, P. Valente, "GEANT4-based full simulation of the PADME experiment at the DAΦNE BTF ", J. Phys. Conf. Ser. 898 (2017) no.4, 042025.

6. M. Raggi *et al.*, "Performance of the PADME Calorimeter prototype at the DAΦNE BTF", Nucl. Inst. Meth. A862 (2017) 31.

7. G. Piperno, "The PADME experiment", Nuovo Cim. C 40, no. 1, (2017) 29.

8. I. Antonova, S. Ceravolo, G. Corradi, G. Georgiev, V. Kozhuharov, M. Mitev, P. Valente, M. Raggi, L. Tsankov, "A Test System for the Front-End Electronics of the PADME charged particle detector system", IEEE Catalog Number CFP17H39-CDR, ISBN 978-1-5386-1752-6, pp.277-280.

References

1. B. Holdom, Phys. Lett. B 166, 196 (1986).
   M. Pospelov, Phys. Rev. D 80, 095002 (2009).

2. M. Raggi and V. Kozhuharov, Rivista del Nuovo Cimento 38 no. 10, (2015).
   DOI 10.1393/ncr/i2015-10117-9

3. I. Valin *et al.*, JINST 7, C01102 (2012).